INTERNATIONAL JOURNAL OF CLIMATOLOGY
Int. J. Climatol. (2013)
Published online in Wiley Online Library
(wileyonlinelibrary.com) DOI: 10.1002/joc.3852

Comparison of NCEP/NCAR and ERA-40 total cloud cover with surface observations over the Tibetan Plateau

Qinglong You,[a]* Yang Jiao,[a] Houbo Lin,[a] Jinzhong Min,[a] Shichang Kang,[b,c] Guoyu Ren[d] and Xianhong Meng[e]

[a] *Key Laboratory of Meteorological Disaster, Ministry of Education, Nanjing University of Information Science and Technology, Nanjing, China*
[b] *State Key Laboratory of Cryospheric Science, Chinese Academy of Sciences (CAS), Lanzhou, China*
[c] *Laboratory of Tibetan Environment Changes and Land Surface Processes, Institute of Tibetan Plateau Research, CAS, Beijing, China*
[d] *Laboratory for Climate Studies, National Climate Center, China Meteorological Administration (CMA), Beijing, China*
[e] *Key laboratory of land surface process and climate change in cold and arid regions, CAS, Lanzhou, China*

ABSTRACT: The annual and seasonal total cloud cover (TCC) variations in the eastern and central Tibetan Plateau (TP) during 1961–2005 are analysed using 71 surface observational stations. The mean TCC decreases from the southeastern to the northwestern TP, consistent with the patterns of atmospheric moisture in the region. The annual mean TCC shows a significant decreasing trend of -0.09 percent decade^{-1}, mainly contributed by winter. About 65% of the stations show significant downward trends on the annual basis with large trend magnitudes occurring in the central TP. The seasonal patterns confirm the annual patterns in most cases. Compared with the surface observations, both National Center for Environmental Prediction/National Center for Atmospheric Research reanalysis (NCEP/NCAR) (1961–2005) and ERA-40 (1961–2001) can reproduce the decreasing TCC trends. The shift of TCC before and after the mid-1980s is obvious in observations and both reanalyses, reflecting the changes of large-scale atmospheric circulation. However, NCEP/NCAR underestimates and ERA-40 overestimates observations on the annual and seasonal basis, presumably caused by the different cloud parameterization schemes. A Taylor diagram diagnose summarizes the discrepancies between observations and reanalyses.

KEY WORDS total cloud cover; NCEP/NCAR and ERA-40; Tibetan Plateau

Received 23 August 2013; Revised 23 September 2013; Accepted 27 September 2013

1. Introduction

Clouds cover about 60% of the Earth's surface, and have great effects on climate change by producing precipitation, reflecting shortwave solar radiation coming from the sun and returning outgoing longwave radiation from the surface (IPCC, 2007). Clouds also act as a blanket similar to that of the greenhouse gases such as water vapour and carbon dioxide, and tend to warm the Earth's surface (IPCC, 2007). Clouds exert great effects on the Earth's radiation budget, and make an important contribution to the greenhouse effect (Wild *et al.*, 2004). There are still large uncertainties about the effects of clouds on climate, which not only depend on cloud height, thickness, horizontal extent and variety, water content, phase (liquid or ice), and the sizes of droplets and crystals, but also rely on the geographical location of the clouds, the albedo and temperature of the underlying surface, and the season of the year and time of day (Warren *et al.*, 2007; Sanchez-Lorenzo *et al.*, 2012).

It is appropriate to investigate the inter-annual variations and trends of clouds, and several studies have analysed clouds at the regional and global scales. Total cloud cover (TCC) shows an increasing trend in the United States during 1976–2004 (Dai *et al.*, 2006), Australia during 1957–2007 (non-significant) (Jovanovic *et al.*, 2011), the former Soviet Union during 1936–1990 (Sun and Groisman, 2000) and Russia during 1991–2010 (Chernokulsky *et al.*, 2011). In other regions and countries, the TCC has decreased including China during 1951–1994 (Kaiser, 1998, 2000), India during 1961–2007 (Jaswal, 2010), most of South Africa during 1960–2005 (Kruger, 2007), and Italy during 1951–1996 (Maugeri *et al.*, 2001). On the other hand, TCC varies from regions, and some parts have increasing trends whereas other regions have decreasing trends, such as Canada during 1953–2003 (Milewska, 2008), Poland during 1971–2000 (Filipiak and Mietus, 2009) as well as the Iberian Peninsula during 1982–2004 (Calbo and Sanchez-Lorenzo, 2009).

The Tibetan Plateau (TP) is the highest and most extensive highland in the world. It is called the 'third Pole', and the cryosphere and climate in the TP are undergoing significant changes caused by global climate

* Correspondence to: Q. You, Key Laboratory of Meteorological Disaster, Ministry of Education, Nanjing University of Information Science and Technology, Nanjing 210044, China. E-mail: yqingl@126.com

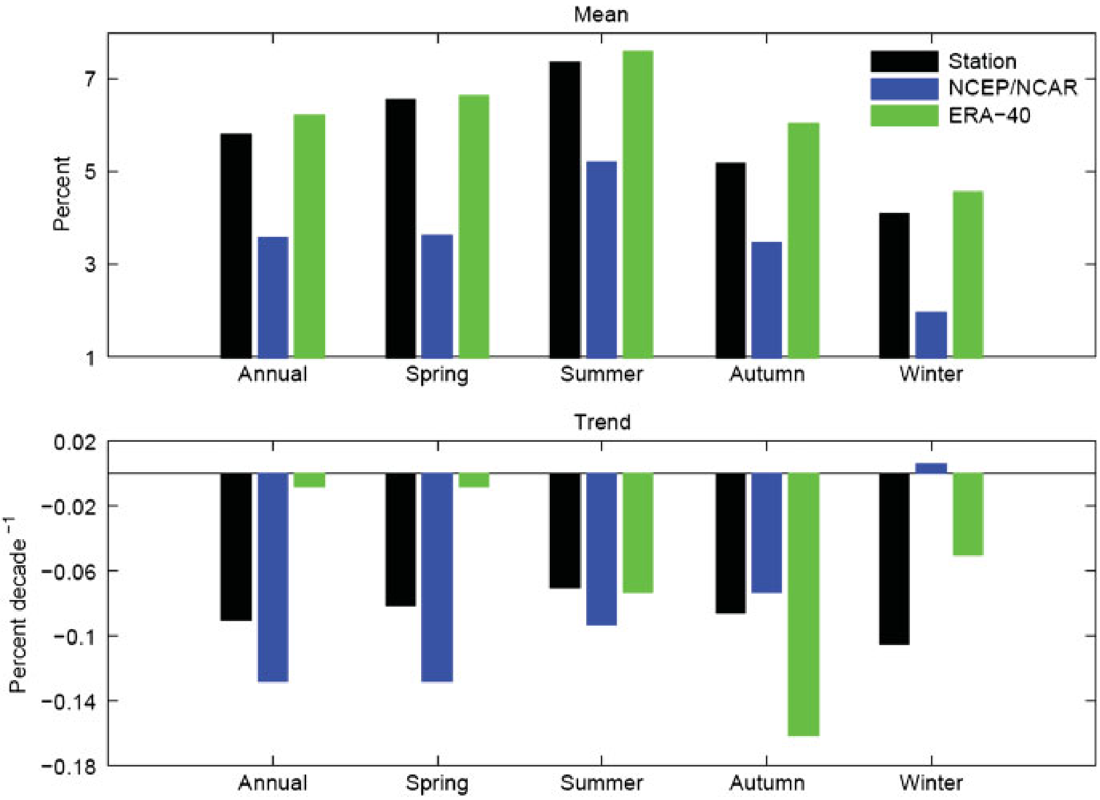

Figure 1. Annual and seasonal means and trends of total cloud cover in the Tibetan Plateau during the period of 1961–2005. The study period for ERA-40 is during 1961–2001.

change (Kang *et al.*, 2010). In the recent years, some meteorological elements in the TP have been investigated by the scientific community, such as extreme temperature changes (You *et al.*, 2008a, 2008b), precipitation (Xu *et al.*, 2008), wind speed (You *et al.*, 2010), surface energy budget in the permafrost (Yao *et al.*, 2011), and cloud (Duan and Wu, 2006). Duan and Wu (2006) found that the low level cloud amount exhibits an increasing trend during the night times, whereas the total and low level cloud amounts display decreasing trends during daytime in the TP during 1961–2003. However, the knowledge of the clouds is limited and largely based on the measurements. The remote sensing products such as ISSCP D2 and MODIS/TERRA have been applied to examine seasonal climatology of high, middle and low clouds in the TP and other regions (Kotarba, 2009; Li *et al.*, 2006; Naud and Chen, 2010). But the evaluations of TCC between observations and reanalyses have not been analysed in detail. In this study, the annual and seasonal (winter: DJF; spring: MAM; summer: JJA; autumn: SON) characteristics of TCC in the eastern and central TP during 1961–2005 are investigated based on the surface observational and reanalyses datasets. Two reanalyses are selected: the National Center for Environmental Prediction/National Center for Atmospheric Research reanalysis (NCEP/NCAR) (Kalnay *et al.*, 1996; Kistler *et al.*, 2001) and the European Centre for Medium-Range Weather Forecasts (ECMWF) reanalysis (ERA-40) (Uppala *et al.*, 2005).

2. Data and methods

Monthly surface TCC data for 71 stations in the TP are provided by the National Meteorological Information Center, China Meteorological Administration (NMIC/CMA). The daily TCC (0–10 tenths of sky cover) is the average of every six hourly observation at the standard synoptic times: 00:00 (midnight), 06:00 (dawn), 12:00 (noon) and 18:00 (dark) at Lhasa Time. The monthly TCC is calculated as daily means averaged four time values. Seventy-one stations were selected according to procedures described in our recent papers (You *et al.*, 2008a, 2008b). Most stations are situated in the eastern and central TP and were installed in 1950s. The elevations of these stations are 2000 m above sea level (a.s.l.) ranging from 2109.5 to 4700 m a.s.l. In order to obtain comparable time series with reanalysis, we selected the data only during 1961–2005 for analysis.

Monthly mean surface TCC from NCEP/NCAR reanalysis is provided by the NOAA/OAR/ESRL PSD, Boulder, CO, USA, from their website at http://www.cdc.noaa.gov/. It covers January 1948 to the present and contains T62 Gaussian grid (192 × 94 points), covering 88.542°N–88.542°S and 0°E–358.125°E (Kalnay *et al.*, 1996; Kistler *et al.*, 2001). It was derived from an empirical relative humidity–cloud cover relationship based on short-range predictions with the operational version of the model (Kalnay *et al.*, 1996; Kistler *et al.*, 2001). The monthly mean surface TCC from ERA-40 reanalysis is obtained from the ECMWF website

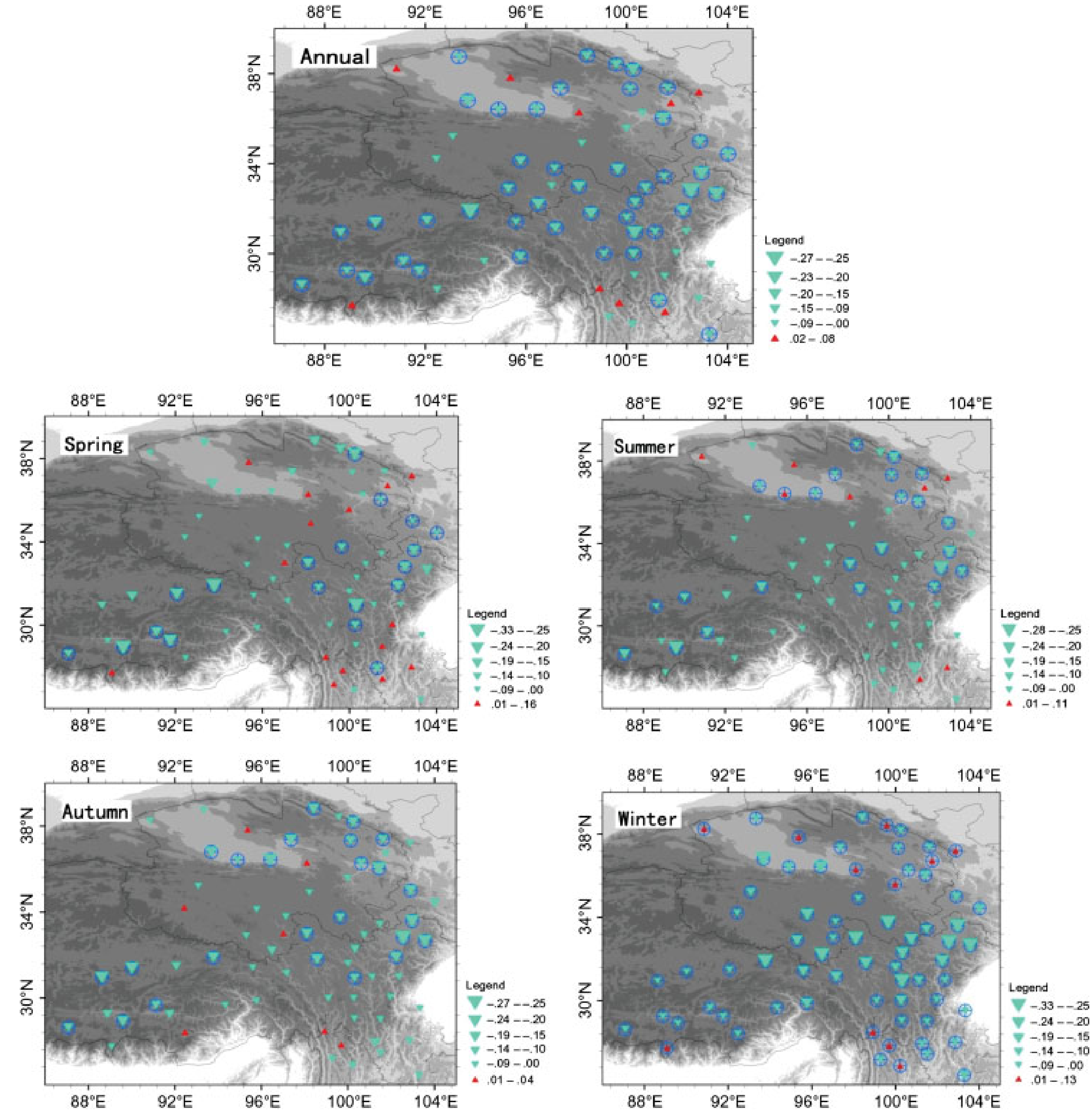

Figure 2. Spatial patterns of trends of annual and seasonal total cloud cover from 71 surface stations in the Tibetan Plateau during 1961–2005. Positive trends are shown as upward triangle, negative trends as downward triangle. The size of the triangle is proportional to the magnitude of the trends. The trends are calculated by the Mann–Kendal methods and trends with the significant level are marked. The unit is percent per decade.

(http://www.ecmwf.int/). ERA-40 reanalysis is available from September 1957 to August 2002 with a spatial resolution of $2.5^\circ \times 2.5^\circ$ (144×73) (Uppala *et al.*, 2005). Previous studies show that the assimilation of satellite humidity data may affect the cloud data in the ERA-40, and this is clear in the tropics and oceans (Betts *et al.*, 2006b; Calbo and Sanchez-Lorenzo, 2009).

The grid datasets (NCEP/NCAR and ERA-40) have different spatial resolutions, and are interpolated to 2.5° horizontal resolution with linear interpolation for easy comparison. After that, grid points of TCC in each reanalysis are interpolated to the 71 observational stations. Periods of 1961–2005 (NCEP/NCAR) and 1961–2001 (ERA-40) are selected. The Mann–Kendall test for trends and Sen's slope estimates are used to detect and estimate trends in annual and seasonal TCC (Sen, 1968), with a significance level defined as $P < 0.05$.

3. Results and comparisons

3.1. TCC from surface station

The regional mean and trend of TCC in the TP on the annual and seasonal basis are shown in Figure 1. Figure 2 shows the spatial patterns of trends of annual and seasonal TCC of the 71 surface stations in the TP during 1961–2005. Positive trends are shown as upward triangle, negative trends as downward triangle. The trends

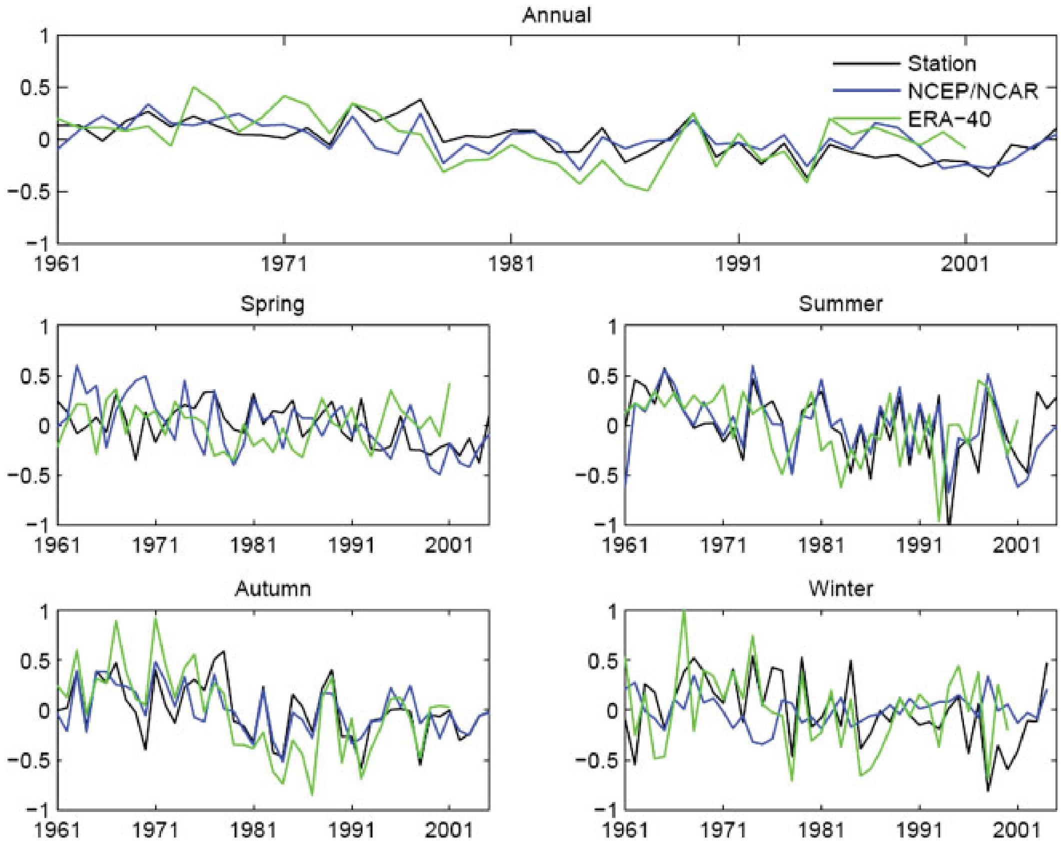

Figure 3. Total cloud cover anomalies from surface stations, NCEP/NCAR and ERA-40 on the annual and seasonal basis in the Tibetan Plateau during 1961–2005.

are calculated by the Mann–Kendal method and those significant ones are marked by circles. The regional anomalies of annual and seasonal mean TCC averaged from 71 surface stations in the TP during 1961–2005 are shown in Figure 3.

Averaging the 71 series available in the TP, the annual mean TCC is 5.81%, with a mean maximum value in summer (7.36%) and a mean minimum value in winter (4.11%). TCC gradually decreases from the southeastern to the northwestern TP with the largest value occurring in the southeastern TP (not shown). This is consistent with the previous studies based on observations during 1971–2004 (Zhang *et al.*, 2008) and International Satellite Cloud Climatology Project C2 dataset (ISCCP-C2) (Wang *et al.*, 2001).

On the annual basis, the mean TCC series in the TP shows a fluctuation before the 1970s and a decreasing trend after that until the 2000s, followed by a statistically significant increasing trend afterwards. Thus, the mean TCC exhibits a significant decreasing trend during 1961–2005 with a rate of −0.090 percent decade^{-1} ($P < 0.05$) (Figure 1). Sixty-two stations have negative trends for TCC, with 46 stations being significant. Stations in the central TP have larger trend magnitudes, while there are still nine stations that have increasing trends in the northern TP. On a seasonal basis, the largest negative trend of TCC is found in winter (−0.104 percent decade^{-1}). The trends for spring, summer, and autumn are −0.081, −0.07, and −0.086 percent decade^{-1}, respectively, and all seasons are statistically significant. Similar to the annual basis, the majority of the stations show a significant decrease, and the patterns of trends are similar to the annual values (Figure 2). Discrepancies on the variation of seasonal TCC trends occur in the central TP with a significant decrease in winter, whereas less pronounced in spring (Zhang *et al.*, 2008).

3.2. TCC from reanalysis data

To compare the TCC variation in the TP with observations, both NCEP/NCAR and ERA-40 reanalysis are derived and interpolated to the 71 stations. Both mean values and trend magnitudes of TCC from NCEP/NCAR and ERA-40 are presented in Figure 1 on the annual and seasonal basis, and the regional anomalies are shown in Figure 3. The spatial patterns of means and trends based on two reanalyses are shown in Figures 4 and 5.

For NCEP/NCAR, the annual mean TCC of 3.57% varies between 2 and 5%, and decreases from the southeastern to the northwestern TP (Figure 4). The pattern of annual mean TCC is similar to observations, but the absolute values are lower in most regions. The annual TCC has a decreasing trend before the 1980s and tends to fluctuate afterwards, with the annual trend of −0.067 percent decade^{-1} during 1961–2005. The decreasing/increasing trend occurs in the southern/northern TP. On the seasonal basis, the largest/smallest mean TCC occurs in

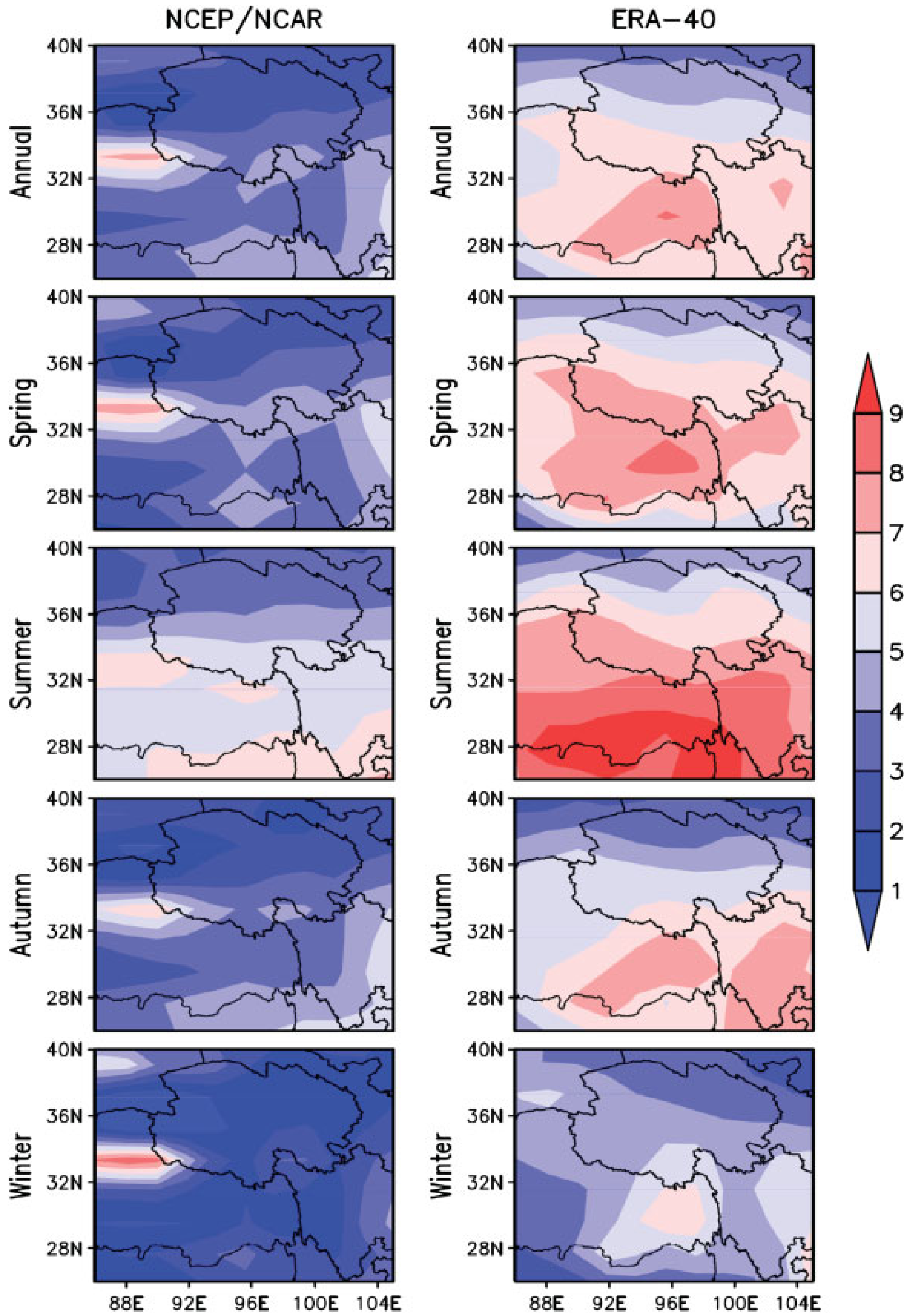

Figure 4. Spatial patterns of mean total cloud cover from NCEP/NCAR during 1961–2005 and ERA-40 reanalysis during 1961–2001 in the Tibetan Plateau on the annual and seasonal basis. The unit is percent.

summer/winter, with the mean values of 5.21 and 1.96%, respectively, consistent with observations. Mean TCC in both spring and autumn is about 3.5%. All seasons with the exception of winter have negative trends, with the largest trend magnitude in spring (−0.128 percent decade^{-1}). The TCC in winter has increased during 1961–2005, profoundly in the northern region, with a mean value of 0.006 percent decade^{-1} (Figure 5).

For ERA-40, the annual mean TCC (6.21%) is larger than the observed mean. The annual mean TCC ranges from 3 to 8%, and larger/smaller mean values occur in the southern/northern TP (Figure 4). Similar to NCEP/NCAR, the annual mean TCC from ERA-40 decreases before the mid-1980s and fluctuates afterwards, leading to a negative trend of −0.085 percent decade^{-1} during 1961–2001. The decreasing trend in the south-eastern TP such as the Sichuan basin is very clear, whereas the western TP has increasing trends. On the seasonal basis, the largest/smallest mean TCC occurs in summer/winter, with the mean values of 7.59 and 4.57%, respectively, which is in accordance with observations and NCEP/NCAR. Mean TCC in spring (6.65%) is

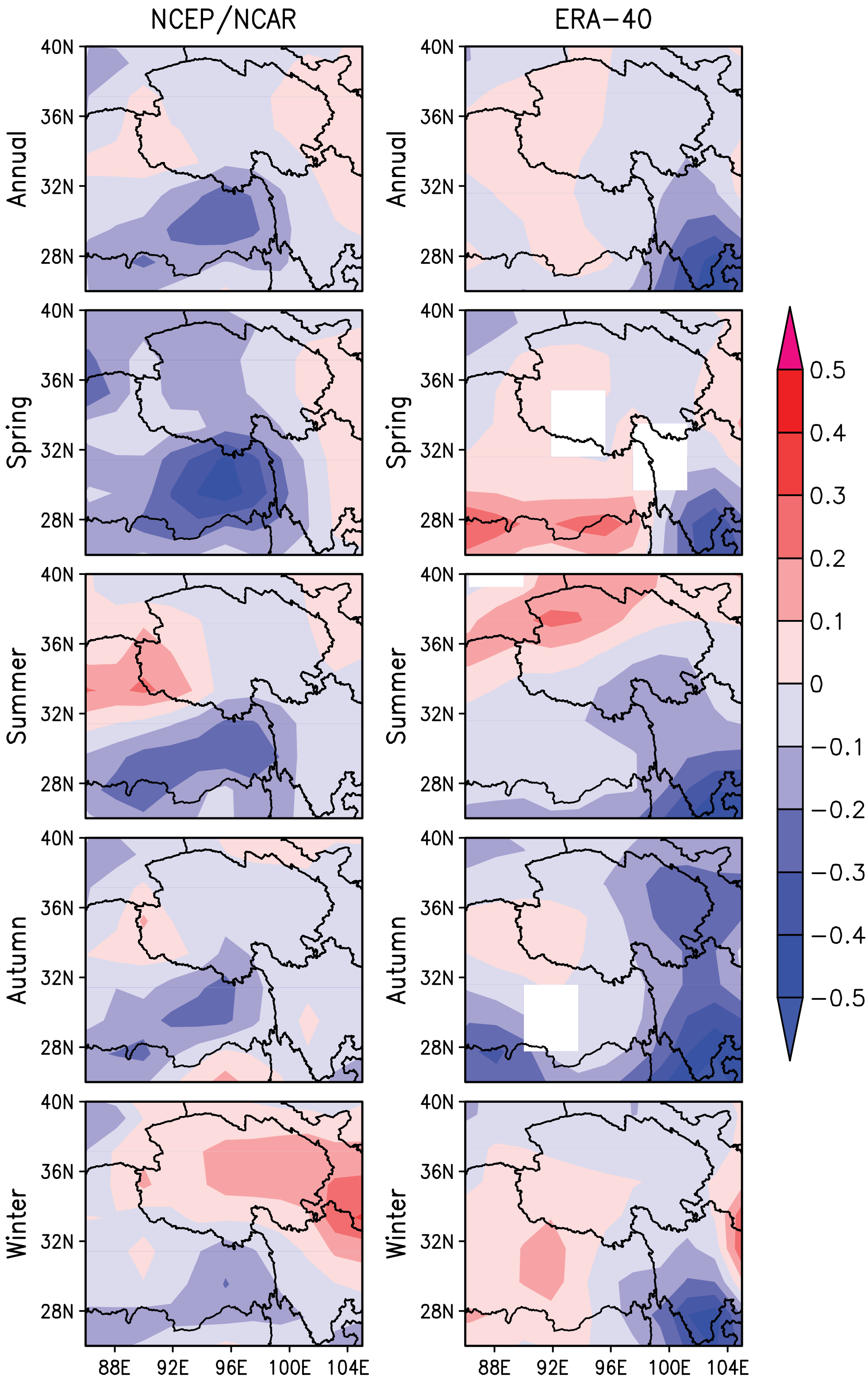

Figure 5. Spatial patterns of trends of annual and seasonal total cloud cover from NCEP/NCAR during 1961–2005 and ERA-40 reanalysis during 1961–2001 in the Tibetan Plateau. The blank area in the ERA-40 means the missing data. The unit is percent per century.

slightly larger than that in autumn (6.03%). TCC of four seasons has decreasing trends, with the largest magnitude in autumn (−0.161 percent decade^{-1}). The trends of TCC in spring, summer, and winter are −0.008, −0.093, and −0.05 percent decade^{-1}, respectively.

3.3. Comparison TCC between observations and reanalyses

To evaluate the TCC from observations, NCEP/NCAR and ERA-40 reanalyses are interpolated to the stations. A Taylor diagram is considered for observations and

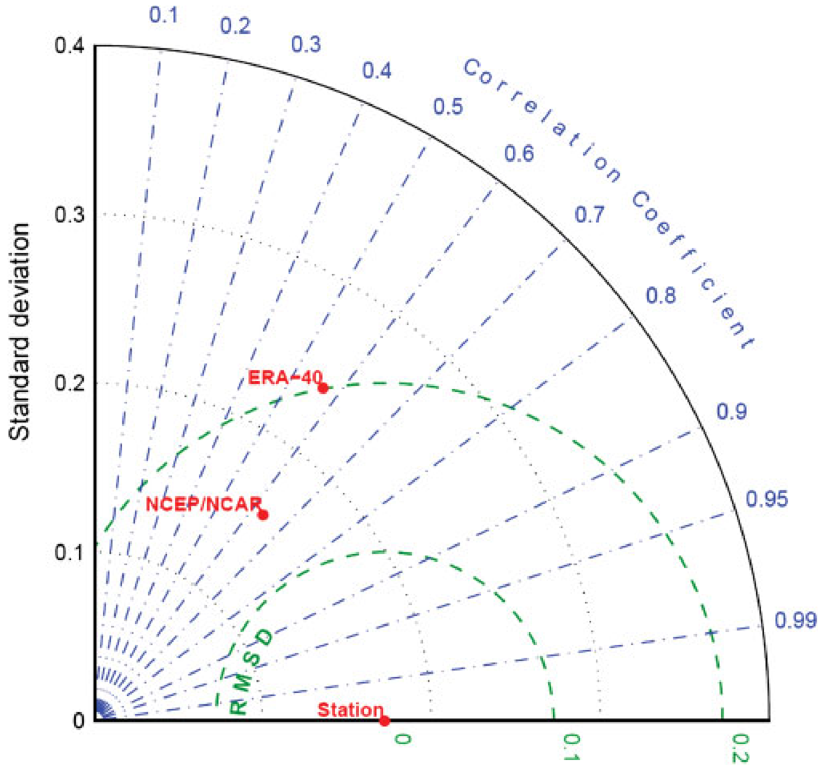

Figure 6. Taylor diagrams showing correlation coefficients, standard deviation, and RMSD of total cloud cover between the surface stations, NCEP/NCAR, and ERA-40 on the annual basis. The radial coordinate is the magnitude of standard deviation, and the concentric semi-circles are the RMSD values. Meanwhile, the angular coordinate shows the correlation coefficient.

reanalyses, which provides a concise statistical summary of how well patterns match each other in terms of their correlation, root mean square difference (RMSD), and the ratio of their variances (Taylor, 2001). Figure 6 shows the correlation coefficients, standard deviation, and the RMSD of TCC between observations, NCEP/NCAR and ERA-40 on the annual basis. The radial coordinate represents the magnitude of standard deviation, the concentric semi-circles are the RMSD values, and the angular coordinate shows the correlation coefficient.

On the annual basis, the mean TCC from observations has positive correlations with NCEP/NCAR and ERA-40 reanalyses, with the correlation coefficients of 0.64 and 0.56, respectively. Taylor diagram analysis reveals that NCEP/NCAR has the lowest standard deviation and smallest root mean square error (RMSE), and captures observations better than ERA-40. For the biases between observations and reanalyses, Taylor diagram has not been used as the visual comparison as reflected in Figure 1. Overall, ERA-40 slightly overestimates observations and NCEP/NCAR underestimates observations on the annual and seasonal basis, while TCC from both reanalyses is in good agreement with the inter-annual variations of observations in the TP.

4. Discussion and conclusions

In this study, the spatial and temporal variations of TCC are analysed based on 71 stations in the eastern and central TP during 1961–2005. In most stations, TCC in the TP has significantly decreasing trends on the annual and seasonal basis (winter: DJF; spring: MAM; summer: JJA; autumn: SON), and a pronounced decrease occurs in winter and autumn. The decreasing TCC was closely connected with recent warming in the TP (Kang *et al.*, 2010). During 1961–2003, TCC and low cloud cover at daytime has decreasing trends in the TP, resulting in more solar radiation and more surface warming. Meanwhile, decreasing TCC and increasing low cloud cover at nighttime also contribute to the nocturnal surface warming (Duan and Wu, 2006).

The mean TCC decreasing from the southeastern to the northwestern TP is controlled by the essential conditions for the formation of clouds, such as water vapour and its condensation (Zhang *et al.*, 2008). Under the influence of the monsoon more water vapour, transported from the ocean and forced to rise, is intercepted by complex topography, which supports conditions to condense from moisture to droplets and cause more clouds in the southern TP. With the weakening of the monsoon and the blocking by topography, less water vapour reaches the northern part, causing fewer clouds in the hinterland TP (not shown).

The decreasing TCC in the TP is in accordance with other studies, such as eastern China (Kaiser, 1998, 2000), India (Jaswal, 2010), South Africa (Kruger, 2007), and Italy (Maugeri *et al.*, 2001). During 1951–1994, most stations in central, eastern and northeastern China show statistically significant decreases of 1–3% sky cover per decade (Kaiser, 1998, 2000). In the previous studies, Zhang *et al.* (2008) concluded that there are two factors accounting for the decreasing TCC in the TP. Firstly, the direct effect of aerosols can be a factor causing for the decreasing TCC. As aerosols can cool the Earth's surface by reflecting sunlight and warm the aerosol layer by absorbing downward longwave radiation, the lapse rate will decrease and atmospheric stability will increase, suppressing cloud formation and reducing the cloudiness (Dai *et al.*, 1997; IPCC, 2007). The TP is regarded as a region with clear atmospheric conditions, and the aerosol amount is sparse (Li *et al.*, 2007; Kang *et al.*, 2010), and can present a clean continental background for the atmospheric composition investigation, such as Nam Co region (Cong *et al.*, 2009). Thus, how the aerosols influence the TCC requires more attention. Secondly, ozone depletion should be another reason for the decreasing TCC in the TP. Previous studies have shown that the ozone depletion in the stratosphere in the TP is confirmed (Zou, 1996; Zhou and Zhang, 2005), which will change the variation of temperature in the middle and upper stratosphere, thus affecting the change of both middle and high level cloud amount. Besides that, cyclonic activity can alter the variations of clouds (Calbo and Sanchez-Lorenzo, 2009). In summary, the mechanism contributing to the decreasing in the TP is unknown and uncertain at present (Zhang *et al.*, 2008).

Both TCC from NCEP/NCAR and ERA-40 are derived to compare with observations and analyse the variability. In the model parameterizations of NCEP/NCAR, a diagnostic cloud scheme has been assimilated, and some tunings of the cloudiness and cloud optical properties have been performed to correct systematic cloudiness errors (Kalnay *et al.*, 1996; Kistler *et al.*, 2001). Meanwhile, a neural-network algorithm (Krasnopolsky *et al.*, 1995) was applied to assimilate SSM/I data after 1987 to improve the clouds (Kalnay *et al.*, 1996; Kistler *et al.*, 2001). Although diagnostic cloud parameterization is made, TCC from NCEP/NCAR underestimates observations on the annual and seasonal basis. ERA-40 assimilation model employs a two-time level semi-Lagrangian advection scheme and a finite element scheme for its vertical discretization, which include improvements of the parameterizations of clouds (Uppala *et al.*, 2005). TCC from ERA-40 overestimates observations on the annual and seasonal basis. This is consistent with the studies in the Iberian Peninsula, especially in its eastern regions where ERA-40 underestimates the clouds due to its underestimation of cyclogenesis in the Mediterranean (Calbo and Sanchez-Lorenzo, 2009). However, the reasons for underestimation of TCC from ERA-40 in the TP need further investigation. Both ERA-40 and NCEP/NCAR reanalyses use their own codes, meteorological profiles, and model fields to compute clouds (Betts *et al.*, 2006a), and there exist discrepancies and uncertainties with observations (Ernst *et al.*, 2007).

Acknowledgements

This study is supported by the National Natural Science Foundation of China (41201072 and 41375015). This study is also funded by the Ministry of Science and Technology of China (Grand No. GYHY201206012) and 'the Priority Academic Program Development of Jiangsu Higher Education Institutions' (PAPD). We are very grateful to the reviewers for their constructive comments and thoughtful suggestions.

References

Betts AK, Zhao M, Dirmeyer PA, Beljaars ACM. 2006a. Comparison of ERA40 and NCEP/DOE near-surface data sets with other ISLSCP-II data sets. *J. Geophys. Res.-Atmos.* **111**: D22S04.

Betts AK, Zhao M, Dirmeyer PA, Beljaars ACM. 2006b. Comparison of ERA40 and NCEP/DOE near-surface data sets with other ISLSCP-II data sets. *J. Geophys. Res.-Atmos.* **111**(D22): D22S04.

Calbo J, Sanchez-Lorenzo A. 2009. Cloudiness climatology in the Iberian Peninsula from three global gridded datasets (ISCCP, CRU TS 2.1, ERA-40). *Theor. Appl. Climatol.* **96**: 105–115.

Chernokulsky AV, Bulygina ON, Mokhov II. 2011. Recent variations of cloudiness over Russia from surface daytime observations. *Environ. Res. Lett.* **6**(3): 035202.

Cong Z, Kang S, Smirnov A, Holben B. 2009. Aerosol optical properties at Nam Co: a remote site in central Tibetan Plateau. *Atmos. Res.* **92**(1): 42–48.

Dai A, DelGenio AD, Fung IY. 1997. Clouds, precipitation and temperature range. *Nature* **386**(6626): 665–666.

Dai A, Karl TR, Sun B, Trenberth KE. 2006. Recent trends in cloudiness over the United States – a tale of monitoring inadequacies. *Bull. Am. Meteorol. Soc.* **87**(5): 597–606.

Duan AM, Wu GX. 2006. Change of cloud amount and the climate warming on the Tibetan Plateau. *Geophys. Res. Lett.* **33**(22): L22704.

Ernst B, Sergey KG, Macke A. 2007. Intercomparison of global cloud cover fields over oceans from the VOS observations and NCEP/NCAR reanalysis. *Int. J. Climatol.* **27**(13): 1707–1719.

Filipiak J, Mietus M. 2009. Spatial and temporal variability of cloudiness in Poland, 1971–2000. *Int. J. Climatol.* **29**(9): 1294–1311.

IPCC. 2007. Summary for Policymakers of Climate change 2007: the physical science basis. In *Contribution of Working Group I to the Fourth Assessment Report of the Intergovernmental Panel on Climate Change*. Cambridge University Press: Cambridge, UK.

Jaswal AK. 2010. Changes in total cloud cover over India based upon 1961–2007 surface observations. *Mausam* **61**(4): 455–468.

Jovanovic B, Collins D, Braganza K, Jakob D, Jones DA. 2011. A high-quality monthly total cloud amount dataset for Australia. *Clim. Change* **108**(3): 485–517.

Kaiser DP. 1998. Analysis of total cloud amount over China, 1951–1994. *Geophys. Res. Lett.* **25**(19): 3599–3602.

Kaiser DP. 2000. Decreasing cloudiness over China: an updated analysis examining additional variables. *Geophys. Res. Lett.* **27**(15): 2193–2196.

Kalnay E, Kanamitsu M, Kistler R, Collins W, Deaven D, Gandin L, Iredell M. 1996. The NCEP/NCAR 40-year reanalysis project. *Bull. Am. Meteorol. Soc.* **77**(3): 437–471.

Kang SC, Xu YW, You QL, Flugel WA, Pepin N, Yao TD. 2010. Review of climate and cryospheric change in the Tibetan Plateau. *Environ. Res. Lett.* **5**(1): 015101.

Kistler R, Collins W, Saha S, White G, Woollen J, Kalnay E. 2001. The NCEP-NCAR 50-year reanalysis: monthly means CD-ROM and documentation. *Bull. Am. Meteorol. Soc.* **82**(2): 247–267.

Kotarba AZ. 2009. A comparison of MODIS-derived cloud amount with visual surface observations. *Atmos. Res.* **92**(4): 522–530.

Krasnopolsky VM, Breaker LC, Gemmill WH. 1995. A neural network as a nonlinear transfer function model for retrieving surface wind speeds from the special sensor microwave imager. *J. Geophys. Res.-Oceans* **100**(C6): 11033–11045.

Kruger AC. 2007. Trends in cloud cover from 1960 to 2005 over South Africa. *Water SA* **33**(5): 603–608.

Li Y, Liu X, Chen B. 2006. Cloud type climatology over the Tibetan Plateau: a comparison of ISCCP and MODIS/TERRA measurements with surface observations. *Geophys. Res. Lett.* **33**: L17716.

Li C, Kang S, Zhang Q, Kaspari S. 2007. Major ionic composition of precipitation in the Nam Co region, Central Tibetan Plateau. *Atmos. Res.* **85**(3–4): 351–360.

Maugeri M, Bagnati Z, Brunetti M, Nanni T. 2001. Trends in Italian total cloud amount, 1951–1996. *Geophys. Res. Lett.* **28**(24): 4551–4554.

Milewska EJ. 2008. Cloud type observations and trends in Canada, 1953–2003. *Atmosphere–Ocean* **46**(3): 297–316.

Naud CM, Chen Y-H. 2010. Assessment of ISCCP cloudiness over the Tibetan Plateau using CloudSat-CALIPSO. *J. Geophys. Res.-Atmos.* **115**: D10203.

Sanchez-Lorenzo A, Calbo J, Wild M. 2012. Increasing cloud cover in the 20th century: review and new findings in Spain. *Climate Past* **8**(4): 1199–1212.

Sen PK. 1968. Estimates of regression coefficient based on Kendall's tau. *J. Am. Stat. Assoc.* **63**: 1379–1389.

Sun BM, Groisman PY. 2000. Cloudiness variations over the former Soviet Union. *Int. J. Climatol.* **20**(10): 1097–1111.

Taylor KE. 2001. Summarizing multiple aspects of model performance in a single diagram. *J. Geophys. Res. Atmos.* **106**(D7): 7183–7192.

Uppala SM, Kållberg PW, Simmon AJ, Andrae U, Bechtold V, Fiorino M. 2005. The ERA-40 re-analysis. *Q. J. Roy. Meteorol. Soc.* **131**(612): 2961–3012.

Wang KL, Hao J, Chen SQ. 2001. Cloud cover over Qinghai-Xizang Plateau: comparison among meteorological station observations, ISCCP-C2, and NCEP reanalysis data. *Plateau Meteor.* **20**(3): 252–257 (in Chinese with English abstract).

Warren SG, Eastman RM, Hahn CJ. 2007. A survey of changes in cloud cover and cloud types over land from surface observations, 1971–96. *J. Climate* **20**(4): 717–738.

Wild M, Ohmura A, Gilgen H, Rosenfeld D. 2004. On the consistency of trends in radiation and temperature records and implications for the global hydrological cycle. *Geophys. Res. Lett.* **31**(11): L11201.

Xu ZX, Gong TL, Li JY. 2008. Decadal trend of climate in the Tibetan Plateau – regional temperature and precipitation. *Hydrol. Processes* **22**(16): 3056–3065.

Yao J, Zhao L, Gu L, Qiao Y, Jiao K. 2011. The surface energy budget in the permafrost region of the Tibetan Plateau. *Atmos. Res.* **102**(4): 394–407.

You QL, Kang SC, Pepin N, Yan YP. 2008a. Relationship between trends in temperature extremes and elevation in the eastern and central Tibetan Plateau, 1961–2005. *Geophys. Res. Lett.* **35**(4): L04704.

You QL, Kang SC, Aguilar E, Yan YP. 2008b. Changes in daily climate extremes in the eastern and central Tibetan Plateau during 1961–2005. *J. Geophys. Res.-Atmos.* **113**(D7): D07101.

You QL, Kang SC, Flugel WA, Pepin N, Yan YP, Huang J. 2010. Decreasing wind speed and weakening latitudinal surface pressure gradients in the Tibetan Plateau. *Climate Res.* **42**(1): 57–64.

Zhang XQ, Peng LL, Zheng D, Tao J. 2008. Cloudiness variations over the Qinghai-Tibet Plateau during 1971–2004. *J. Geogr. Sci.* **18**: 142–154.

Zhou SW, Zhang RH. 2005. Decadal variations of temperature and geopotential height over the Tibetan Plateau and their relations with Tibet ozone depletion. *Geophys. Res. Lett.* **32**(18): L18705.

Zou H. 1996. Seasonal variation and trends of TOMS ozone over Tibet. *Geophys. Res. Lett.* **23**(9): 1029–1032.

